

Cytoplasmic p21^{Cip1} Is Involved in Ras-induced Inhibition of the ROCK/LIMK/Cofilin Pathway*

Received for publication, June 30, 2003, and in revised form, October 3, 2003
Published, JBC Papers in Press, October 14, 2003, DOI 10.1074/jbc.M306968200

Sungwoo Lee^{‡§} and David M. Helfman^{‡¶}

From the [‡]Cold Spring Harbor Laboratory, Cold Spring Harbor, New York 11724 and the [§]Department of Molecular Genetics and Microbiology, State University of New York, Stony Brook, New York 11794

Accumulating evidence suggests that p21^{Cip1} located in the cytoplasm might play a role in promoting transformation and tumor progression. Here we show that oncogenic H-RasV12 contributes to the loss of actin stress fibers by inducing cytoplasmic localization of p21^{Cip1}, which uncouples Rho-GTP from stress fiber formation by inhibiting Rho kinase (ROCK). Concomitant with the loss of stress fibers in Ras-transformed cells, there is a decrease in the phosphorylation level of cofilin, which is indicative of a compromised ROCK/LIMK/cofilin pathway. Inhibition of MEK in Ras-transformed NIH3T3 results in restoration of actin stress fibers accompanied by a loss of cytoplasmic p21^{Cip1}, and increased phosphorylation of cofilin. Ectopic expression of cytoplasmic but not nuclear p21^{Cip1} in Ras-transformed cells was effective in preventing stress fibers from being restored upon MEK inhibition and inhibited phosphorylation of cofilin. p21^{Cip1} was also found to form a complex with ROCK in Ras-transformed cells *in vivo*. Furthermore, inhibition of the PI 3-kinase pathway resulted in loss of p21^{Cip1} expression accompanied by restoration of phosphocofilin, which was not accompanied by stress fiber formation. These results suggest that restoration of cofilin phosphorylation in Ras-transformed cells is necessary but not sufficient for stress fiber formation. Our findings define a novel mechanism for coupling cytoplasmic p21^{Cip1} to the control of actin polymerization by compromising the Rho/ROCK/LIMK/cofilin pathway by oncogenic Ras. These studies suggest that localization of p21^{Cip1} to the cytoplasm in transformed cells contributes to pathways that favor not only cell proliferation, but also cell motility thereby contributing to invasion and metastasis.

p21^{Cip1/Waf1} (hereafter referred to as p21) is best known for its ability to directly block the kinase activities of a broad range of cyclin/cyclin-dependent kinase (CDK)¹ complexes in response to anti-mitogenic signals or DNA damage (1–3). Despite

* The costs of publication of this article were defrayed in part by the payment of page charges. This article must therefore be hereby marked "advertisement" in accordance with 18 U.S.C. Section 1734 solely to indicate this fact.

¶ Supported by Grant CA83182 from the National Cancer Institute. To whom correspondence should be addressed: Cold Spring Harbor Laboratory, 1 Bungtown Rd., Cold Spring Harbor, NY 11724. Tel.: 516-367-8838; Fax: 516-367-8815; E-mail: helfman@cshl.edu.

¹ The abbreviations used are: CDK, cyclin-dependent kinase; ROCK, Rho kinase; LIMK, LIM kinase; MEK, mitogen-activated protein kinase kinase; ERK, extracellular signal-regulated kinase; PI3K, phosphatidylinositol 3-kinase; NLS, nuclear localization signal; EGFP, enhanced green fluorescence protein; Cip, CDK inhibitory protein; Kip, kinase inhibitory protein; mAb, monoclonal antibody; Me₂SO, dimethyl sulfoxide; DAPI, 4',6-diamidino-2-phenylindole; TM, tropomyosin; HMW, high molecular weight.

its function as a cell cycle inhibitor, which implies that p21 is a tumor suppressor, elevated level of p21 in the cytoplasm has been reported to be critical for promoting cell transformation and survival (4–8). Strikingly, the level of p21 expression is highly increased in various human cancers such as breast cancer, bladder cancer, pancreatic cancer, and glioblastoma (9–12). It remains unclear how elevated cytoplasmic p21 might contribute to tumorigenesis. One possibility is that p21 is sequestered away from the nucleus in transformed cells thereby preventing it from binding to nuclear cyclin/CDK complexes, thus allowing sufficient cyclin/CDK activity for cell cycle progression (13). Alternatively, relocalization of p21 to the cytoplasm may target cytoplasmic molecules such as apoptosis signal-regulating kinase 1 (ASK1) thereby promoting cell survival (7).

The Rho family of GTPases, Rho, Rac, and Cdc42, regulate cell morphology, cytokinesis, and cell motility through reorganization of actin filaments (14). The interplay between these GTPases plays a critical role in the regulation of cell morphology and motility. Activation of Rac enhances cell spreading and migration by stimulation of actin polymerization at the plasma membrane and promoting lamellipodia formation. By contrast, Rho stimulates contractility and adhesion by inducing the formation of actin stress fibers and focal adhesions. Rho cycles between GDP-bound inactive and GTP-bound active forms, and the GTP-bound form binds to specific targets to exert its biological functions. Two closely related Rho kinases, ROCK-I and -II, have been established to be key downstream effectors of Rho to form stress fibers and focal adhesions (15). Rho kinases contribute to the increased actin-myosin II-mediated contractility by directly phosphorylating myosin light chain (MLC) and negatively regulate myosin light chain phosphatase (MLCP) by phosphorylating myosin binding subunit (MBS) of MLCP (16, 17). Rho kinases also activate LIM kinase, which subsequently phosphorylates cofilin and thereby inhibits its actin-depolymerizing activity, thus leading to stabilization of actin stress fibers (18).

Ras (H-Ras, K-Ras, N-Ras) regulates cell growth, differentiation, and cell motility (14). The frequency of Ras mutations is one of the highest of any gene in human cancers (19). Cells transformed by oncogenic Ras are characterized not only by deregulated growth control but also pronounced alterations in the organization of the actin cytoskeleton and adhesive interactions. Changes in the organization of actin filaments are highly correlated with anchorage-independent growth and tumorigenicity, suggesting a fundamental role for actin fibers in cell growth control (20–22). We and others (23, 24) have shown that transformation of fibroblasts cells by oncogenic Ras induces constitutive activation of MEK, which causes disruption of actin cytoskeleton by inactivating the Rho-ROCK-LIM kinase pathway. The inhibition of Rho-dependent stress fiber formation contributes to the increased motility of Ras-trans-

formed fibroblasts (24). However, the mechanism of this inactivation has not been elucidated.

In this study, we show that cytoplasmic p21 plays a critical role in the morphological and cytoskeletal changes observed in Ras-transformed fibroblasts. We demonstrate that sustained activation of both MEK and PI3K effector pathways are necessary for the elevation of p21 protein in the cytoplasm of Ras-transformed NIH3T3 cells. The cytoplasmic p21 forms a physical complex with ROCK and inhibits its activity, thereby contributing to the loss of actin stress fibers by compromising the ROCK/LIMK/cofilin pathway. Our findings suggest a novel physiological role for cytoplasmic p21 in remodeling of the actin cytoskeleton by oncogenic Ras.

EXPERIMENTAL PROCEDURES

Antibodies and Reagents—The mouse monoclonal anti-ROCK-I mAb (clone 46) and anti-ROCK-II mAb (clone 21) were purchased from Transduction Laboratories (Lexington, KY). Anti-p21^{Cip1} mAb and rabbit polyclonal antibody detecting cofilin phosphorylated by LIMK at Ser-3 was from Santa Cruz Biotechnology (Santa Cruz, CA). Monoclonal anti-vinculin antibody (hVIN-1) was from Sigma Chemical. The rabbit polyclonal anti-cofilin was from Cytoskeleton (Denver, CO). The rabbit anti-ROCK-I pAb was kindly provided by Dr. Jian Du in Dr. Greg Hannon's laboratory (Cold Spring Harbor Laboratory, NY). Secondary antibodies Cy3-conjugated goat anti-mouse and goat anti-rabbit IgG were purchased from Jackson ImmunoResearch Laboratories (West Grove, PA). Oregon green-conjugated and rhodamine-conjugated phalloidins were from Molecular Probes (Eugene, OR). U0126, LY294002, and Y27632 were from Calbiochem (La Jolla, CA). All tissue culture reagents were from Invitrogen.

Cell Culture and Retroviral Infection—Normal NIH3T3 cells were obtained from the Tissue Culture Facility of Cold Spring Harbor Laboratory. Cells were maintained in Dulbecco's modified Eagle's medium containing 10% BCS, 100 units/ml penicillin, and 100 µg/ml streptomycin in a humidifier air (5% CO₂) atmosphere, at 37 °C. The stable cell line expressing H-RasV12 was obtained by the following protocol: pWZL-Hygro H-RasV12 and corresponding empty retroviral vector were used to transfect the ecotropic packaging cell line φNX. Transfection was performed by the calcium phosphate method. At 72 h post-transfection, viral supernatants were collected, filtered, and supplemented with 4 µg/ml polybrene. The supernatant was then used to infect NIH3T3 cells. After infection, cells were selected in hygromycin (50 µg/ml) for 14 days.

Plasmids and Transfection—Retroviral pWZL-Hygro H-RasV12 vector was a generous gift of Yvette Seger in the Hannon laboratory (Cold Spring Harbor Laboratory). pEGFP-full-length-p21 (amino acids 1–164) and pEGFP-ΔNLS-p21 (amino acids 1–140) were provided by Dr. Minoru Asada (International Medical Center of Japan). pEGFP-N1-XAC, expressing wild-type *Xenopus* cofilin tagged with EGFP at the C terminus, was kindly provided by James Bamburg (Colorado State University). For transient transfection, cells were grown at 60–70% confluency in Dulbecco's modified Eagle's medium containing 10% BCS. Cells were transfected with a total of 2 µg of expression vectors per dish, using LipofectAMINE PLUS reagent (Invitrogen) according to the manufacturer's protocol. At 24 h post-transfection, cells were split and plated onto glass coverslips followed by incubation for additional 24 h. In some cases, cells on the coverslips were treated with Me₂SO, U0126, or LY294002 for various time periods, then the coverslips were harvested and processed for immunofluorescence.

Immunofluorescence—Cells grown on glass coverslips were fixed with 3% paraformaldehyde for 15 min, permeabilized with 0.2% Triton X-100 for 5 min, then blocked for 30 min with 1% bovine serum albumin/phosphate-buffered saline at room temperature. For immunofluorescence, fixed cells were incubated for 1 h with mouse monoclonal p21 antibody (Santa Cruz Biotechnology) or monoclonal vinculin antibody followed by Cy3-conjugated goat anti-mouse IgG for 1 h. To visualize F-actin, Oregon green, or rhodamine-conjugated phalloidin (1:100) was diluted in 1% bovine serum albumin/phosphate-buffered saline for staining. The coverslips were stained with 4'6-diamidino-2-phenylindole (DAPI), and then mounted using Prolong Antifade (Molecular Probes). Samples were examined, and pictures were acquired on a Zeiss Axiophot microscope equipped with a Photometrics Sensys (Oberkochen, Germany) cooled CCD camera using Openlab 3.1.1 software. All photographs were taken at the same magnification.

Immunoprecipitation and Western Blot Analysis—Cell lysates were prepared as previously described in 50 mM Tris-HCl, pH 7.5, 150 mM

NaCl, 10% glycerol, 0.5% Nonidet-P40 including protease inhibitor mixture tablets (Roche Applied Science) (8). The cell lysates were centrifuged at 13,000 × g for 20 min, and the supernatant was collected. Immunoprecipitations were performed for 1 h at 4 °C using polyclonal anti-ROCK-I antibody. The immunocomplexes were collected with protein G-Sepharose (Amersham Biosciences) slurry (50% v/v), washed four times with lysis buffer, and subjected to SDS-PAGE. For Western blot, control and treated cells were washed with ice-cold phosphate-buffered saline containing 1 mM sodium orthovanadate before direct extraction in 2× SDS Laemmli Sample Buffer. Lysates were clarified by centrifugation (16,000 × g for 15 min at 4 °C), and protein concentrations were measured by Bradford assay (Bio-Rad, Hercules, CA). 10 µg of proteins were resolved by SDS-PAGE then transferred to nitrocellulose membrane (Schleicher & Schuell, Keene, NH). The membrane was blocked for 30 min in 5% nonfat dried milk or 1% bovine serum albumin in phosphate-buffered saline plus 0.1% Tween 20 and incubated with primary antibodies for 1 h, followed by incubation with appropriate horseradish peroxidase-conjugated secondary antibodies for 1 h at room temperature. Immunoreactive bands were detected by chemiluminescence (PerkinElmer Life Sciences).

Rho-GTP Pull-down Assay—Measurement of GTP-bound Rho was performed using the Rho Activation Assay kit (Upstate Biotechnology), following the manufacturer's instructions. Briefly, the RhoA-binding domain of Rhotekin expressed as a GST fusion protein was used to affinity precipitate GTP-bound Rho from cells lysed in 50 mM Tris, pH 7.2, 1% Triton X-100, 0.5% sodium deoxycholate, 0.1% SDS, 500 mM NaCl, 10 mM MgCl₂, and protease inhibitor mixture (Roche Applied Science). Precipitated Rho-GTP was then detected by immunoblot analysis, using a monoclonal anti-RhoA antibody (Santa Cruz Biotechnology).

RESULTS

Ras Uncouples Rho-GTP from the ROCK/LIMK/Cofilin Pathway—NIH3T3 fibroblasts have a flat morphology and well-developed stress fibers, whereas cells transformed by H-RasV12 are rounded and lack stress fibers (Fig. 1A). RasV12 is known to activate several effector pathways including Raf/MEK/MAP, phosphatidylinositol 3-kinase (PI3K), and RalGDS (25–27). To dissect which signaling pathway is necessary for the prevention of stress fiber formation in Ras-transformed NIH3T3 cells, we treated Ras-transformed cells with U0126 or LY294002, which specifically inhibit MEK or PI3K, respectively. We found that the disruption of stress fibers and focal adhesions observed in Ras-transformed cells were reversed by treatment with U0126 but not by LY294002 (Fig. 1A). These observations are in agreement with previous studies that showed that activation of the MEK-dependent pathway, but not PI3K, is necessary for disruption of the actin stress fibers and focal adhesions by oncogenic Ras (23, 24). We also observed that the restoration of stress fibers and focal adhesions by U0126 requires ROCK activity, because either dominant negative ROCK-I or the ROCK inhibitor, Y27632, were able to prevent stress fiber formation caused by U0126 (data not shown).

The small GTPase, RhoA, is known to act upstream of ROCK and induce the formation of stress fibers and focal adhesions (14). To examine whether the cytoskeletal changes induced by Ras oncogene were elicited by regulation of RhoA activity, we measured the levels of Rho-GTP, using an assay that only captures the active GTP-bound form of the GTPase (28). Although three isoforms of Rho protein were described, we measured only RhoA-GTP, because neither RhoB nor RhoC were detectable in NIH3T3 (data not shown). The level of RhoA-GTP in Ras-transformed cells was higher than that in parental NIH3T3 (Fig. 1B), but the difference was abolished by U0126, consistent with the results obtained by others (29) that sustained activation of Raf/MEK/ERK pathway is required for the activation of RhoA protein. More importantly, these data demonstrate that active RhoA-GTP, despite its increased level, is no longer coupled via its interaction with ROCK to the formation of stress fibers in Ras-transformed cells.

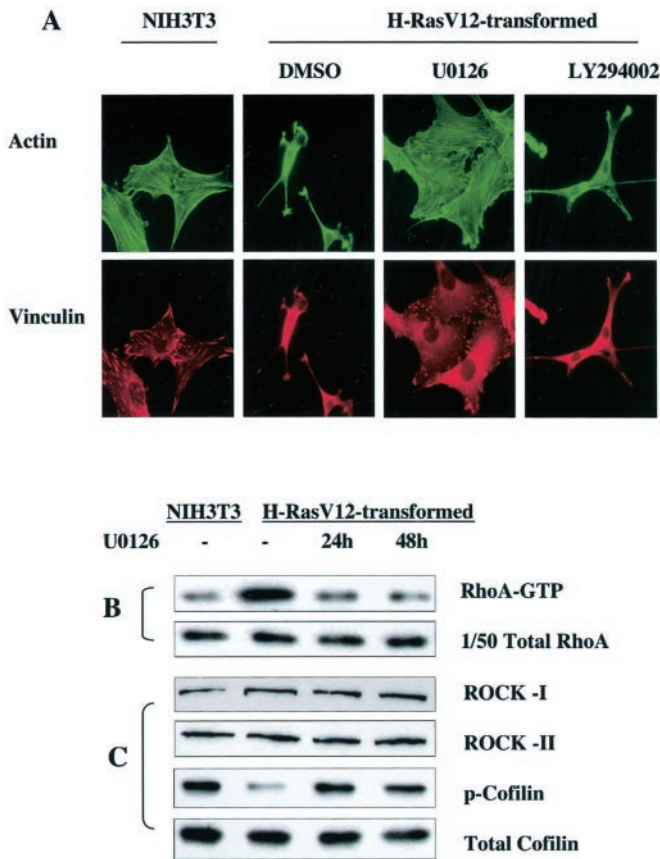


FIG. 1. RhoA-GTP fails to activate Rho kinases in H-RasV12 transformed NIH3T3 cells. Untransformed or Ras-transformed NIH3T3 cells were cultured overnight. The cells were then treated with U0126 (25 μ M), LY294002 (50 μ M), or Me₂SO (DMSO, 0.1% v/v) for 24 h followed by immunofluorescence or Rho-GTP assay or Western blot. *A*, cells were stained for F-actin to visualize the cytoskeleton and vinculin to visualize focal adhesions using Oregon green-conjugated phalloidin and anti-vinculin antibody, respectively. All photographs were taken at the same magnification. *B*, cell lysates were subjected to the Rho activity assay and the amount of Rhotekin-bound Rho (active) and total Rho was analyzed by anti-RhoA antibody. Similar results were obtained in three independent experiments. *C*, cell lysates were analyzed to measure the amounts of ROCK-I, -II, phosphorylated cofilin, and total cofilin by Western blot (representative of three independent experiments).

It was previously reported that a MEK-dependent pathway leads to disorganization of the actin cytoskeleton in Ras-transformed fibroblasts by down-regulation of ROCK-I/II protein expression (23, 24). In these studies, they showed that the amount of Rho-GTP in Ras-transformed cells was comparable to or higher than that of the untransformed control cells. Therefore, we also compared the levels of ROCK-I/II proteins between untransformed and Ras-transformed NIH3T3 cells. No changes in the levels of either ROCK-I or -II proteins were detected (Fig. 1C). ROCK-I/II can activate LIM kinase, which in turn phosphorylates cofilin and thereby inhibits its actin-depolymerizing activity, thus leading to stabilization of stress fibers (30, 31). To determine if Ras causes any decrease in phosphorylated cofilin in NIH3T3 cells, we used an antibody that detects cofilin phosphorylated by LIM kinase at the Ser-3 residue. We found that cofilin phosphorylation was significantly decreased by expression of Ras (Fig. 1C). Furthermore, the level of phosphorylated cofilin was restored following treatment of Ras-transformed cells with the MEK inhibitor (Fig. 1C). These results indicate an alternative mechanism exists, other than a decrease in ROCK-I/II proteins as previously reported in Ras-transformed NRK and Swiss 3T3 cells (23, 24), for uncoupling Rho-GTP from activating Rho kinases.

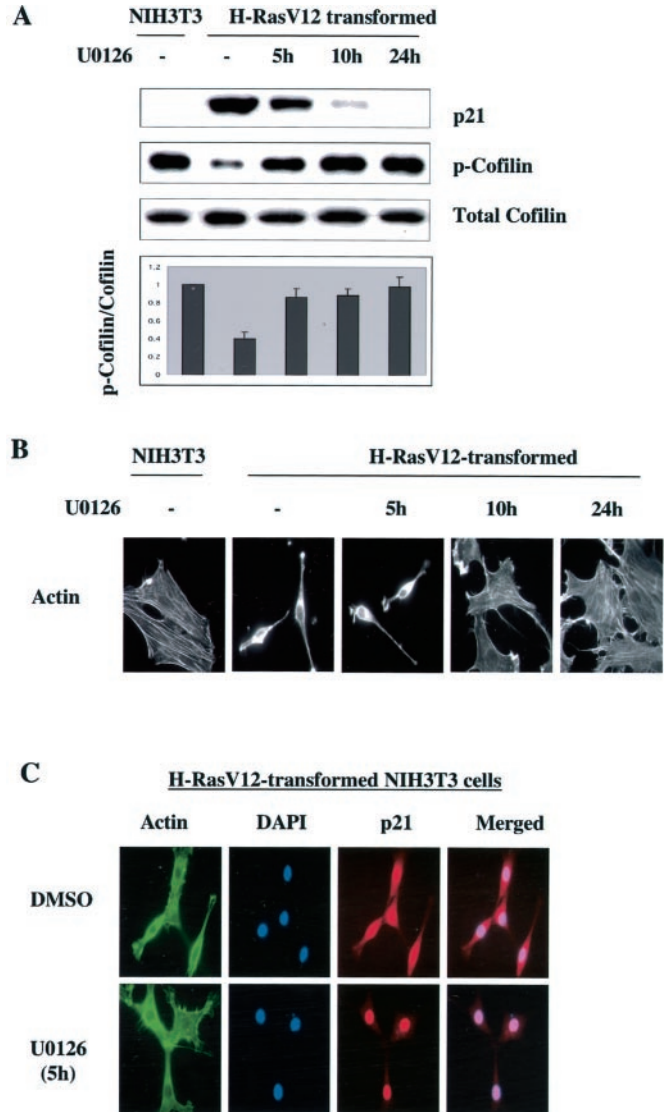


FIG. 2. The amount of p21 correlates inversely with the formation of stress fibers. Parental NIH3T3 and Ras-transformed cells were grown overnight and then treated with Me₂SO (DMSO, 0.1% v/v) or 25 μ M U0126 for the indicated times. *A*, whole cell lysates were immunoblotted with anti-p21, anti-phosphocofilin, and anti-cofilin antibodies. Western blot for total cofilin was done after membrane stripping. Levels of cofilin phosphorylation were estimated by densitometry using an image analyzer (AlphaImager 2200 version 5.5 software). Relative cofilin phosphorylation levels, normalized to total cofilin, are expressed versus control cells, which are arbitrarily set to 1. Each value represents the mean \pm S.D. of three independent experiments. *B*, cells grown overnight on coverslips were treated with 0.1% Me₂SO or 25 μ M U0126 for various time periods as indicated, then fixed and stained with Oregon green-conjugated phalloidin. *C*, Ras-transformed cells were treated with 0.1% Me₂SO (DMSO, control) or 25 μ M U0126 (5 h), then fixed and stained with phalloidin, DAPI, and anti-p21 antibody.

Elevated Levels of Cytoplasmic p21 Correlates with the Disruption of Stress Fibers in Ras-transformed Cells—Despite its implied role as a tumor suppressor, the level of p21 protein is significantly elevated in many types of human cancer (2). In agreement with these observations, we found that p21 protein expression is induced by Ras in NIH3T3 cells (Fig. 2A). This is consistent with recent studies showing that Ras activates p21 transcription and promotes p21 protein stability via blocking proteasome-mediated degradation (32, 33). The p21 protein was decreased in Ras-transformed cells by MEK inhibition in a time-dependent manner (Fig. 2A). It was completely undetectable at 24 h post-treatment of U0126. This demonstrates that

the increase in expression of p21 protein in Ras-transformed cells was dependent on sustained activation of the Raf/MEK/ERK pathway. Interestingly, the decrease of p21 following U0126 treatment was temporally associated with the restoration of stress fibers and increase in cofilin phosphorylation (Fig. 2, A and B). These observations suggested an inverse relationship between the concentration of p21 protein and the formation of stress fibers. Recently, it was reported that p21 is induced in the cytoplasm during neuronal differentiation and is involved in blocking Rho-induced actin remodeling leading to neurite outgrowth (8). To determine if cytoplasmic p21 was involved in remodeling of the actin cytoskeleton in Ras-transformed NIH3T3 cells, we performed immunofluorescence staining to determine the localization of p21. We found that in 90% of Ras-transformed cells p21 exists abundantly in the cytoplasm as well as in the nucleus (Fig. 2C), whereas p21 was not detectable in the majority of asynchronous NIH3T3 cells (data not shown), which is consistent with our Western blot data (Fig. 2A). However, the p21 protein became barely detectable in the cytoplasm of 70% Ras-transformed cells if treated with the MEK inhibitor for 5 h (Fig. 2C). Concomitant with a decrease in cytoplasmic p21, at 5 h post-treatment of U0126, there was an increase in the levels of phosphorylated cofilin, although it was too early to monitor obvious reassembly of stress fibers (Fig. 2, A and B). These results suggest that the loss of p21 from the cytoplasm and restoration of cofilin phosphorylation might be associated with MEK inhibition-mediated reassembly of stress fibers.

Cytoplasmic p21 Is Sufficient for the Maintenance of Disorganized Stress Fibers in Ras-transformed Cells—To directly determine whether the expression of cytoplasmic p21 is sufficient to block stress fiber formation in Ras-transformed cells, we transfected Ras-transformed cells with either a full-length p21 or p21 with a deletion in the nuclear localization signal (NLS). Following 48 h post-transfection, we treated the cells with U0126 for an additional 24 h, which caused complete loss in the expression of endogenous p21 but not in that of exogenous p21 (data not shown). Therefore, we could determine if ectopic expression of Δ NLS-p21 would affect the restoration of stress fibers by the MEK inhibitor. Ectopic expression of either Δ NLS-p21 or full-length p21 had no effect on the morphology of Ras-transformed cells in the absence of U0126 (Fig. 3A). However, 88% (44/50) of cells expressing the EGFP- Δ NLS-p21 in the cytoplasm were refractory to the restoration of stress fibers caused by MEK inhibition, whereas most of cells expressing the EGFP control or EGFP-full-length p21 in the nucleus failed to show such a resistance (Fig. 3B). We also observed that exogenous p21, but not Δ NLS-p21, relocalized to the nucleus similarly as endogenous p21 following MEK inhibition (Figs. 2C and 3B), confirming that cytoplasmic p21, but not nuclear, conferred such a refractory effect. Furthermore, ectopic expression of Δ NLS-p21, but not full-length p21, was sufficient to cause disruption of the actin cytoskeleton in 47% (39/83) of untransformed NIH3T3 cells (Fig. 3C). It is noteworthy that full-length p21 showed nuclear-specific pattern of expression in 90% of transfectants, implying that p21 is normally localized in the nucleus under the absence of oncogenic Ras activation. Collectively, these results suggest that localization of p21 to the cytoplasm by Ras is involved in reorganization of the actin cytoskeleton.

In Vivo Interaction of p21^{Cip1} with ROCK—ROCK is known to act downstream of Rho to induce stress fiber formation in fibroblasts (15). In one report, the expression of cytoplasmic p21 promotes neurite outgrowth in hippocampal neurons by forming complex with ROCK and inhibiting its activity (8). To determine whether endogenous p21 physically interacts with

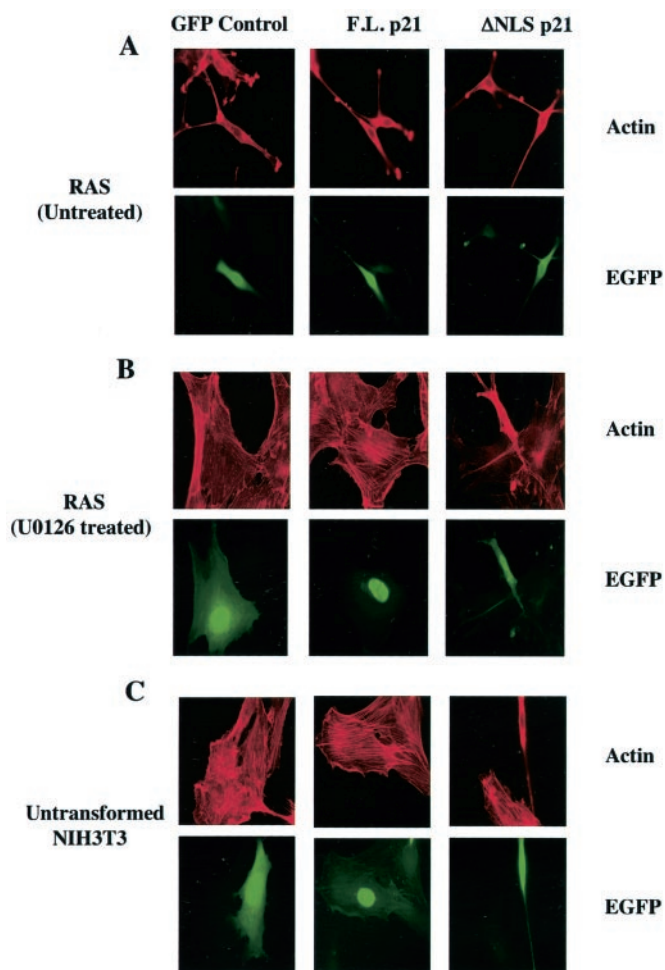


Fig. 3. Cytoplasmic p21 is involved in the disruption of stress fibers. H-RasV12-transformed NIH3T3 (A and B) or control NIH3T3 (C) were transiently transfected with empty-EGFP control, EGFP-full length p21, and EGFP- Δ NLS-p21 constructs. After 48 h, cells were fixed without drug treatment (C) or maintained in the absence (A) or presence (B) of 25 μ M U0126 for additional 24 h followed by fixation. F-actin was visualized using rhodamine-conjugated phalloidin (top panels; A–C). EGFP-expressing cells represent transfectants (bottom panels; A–C).

ROCK *in vivo*, we immunoprecipitated ROCK from Ras-transformed NIH3T3 cells in which p21 is highly expressed. We found that endogenous p21 was coprecipitated with an anti-ROCK-I antibody (Fig. 4A), demonstrating that endogenous p21 forms a complex with ROCK-I *in vivo*. Next, we sought to determine whether ectopic expression of cytoplasmic p21 in NIH3T3 cells could directly interfere with ROCK/LIMK/cofilin pathway. For this purpose, we measured the level of phosphorylation of exogenously expressed cofilin after cotransfecting EGFP-tagged cofilin in combination with Δ NLS-p21 or controls. The phosphorylation of exogenous EGFP-cofilin was significantly reduced by Δ NLS-p21 protein but not by the wild-type p21 (Fig. 4B). In addition, treatment of a specific ROCK inhibitor, Y27632 (10 μ M), effectively blocked the phosphorylation of EGFP-cofilin, an observation consistent with the notion that endogenous ROCK is an upstream effector mediating LIM kinase-dependent phosphorylation of exogenous EGFP-cofilin as well (Fig. 4B). Taken together, these results suggest that association of p21 with ROCK in the cytoplasm is the mechanism by which ROCK/LIMK/cofilin pathway is compromised in Ras-transformed cells.

Restoration of Cofilin Phosphorylation by Inhibition of PI3K Is Not Sufficient for Stress Fiber Formation—There is increas-

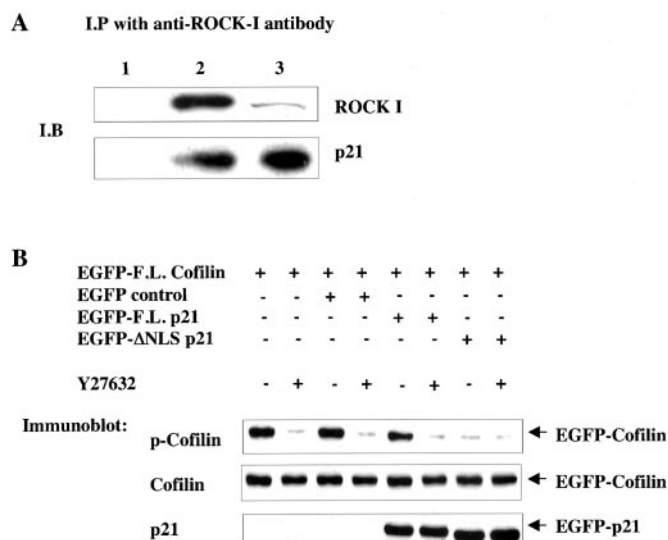


FIG. 4. Cytoplasmic p21 interacts with ROCK and inhibits cofilin phosphorylation. *A*, cell lysates of Ras-transformed cells were immunoprecipitated with a polyclonal anti-ROCK-I antibody (lane 2) or preimmune serum (lane 1) as a negative control. Immunocomplexes were then electrophoresed followed by blotting with anti-ROCK-I (top) or anti-p21 antibody (bottom). Whole cell lysate from Ras-transformed cells was used for positive size marker of ROCK-I and p21 (lane 3). *B*, NIH3T3 cells were cotransfected with EGFP-cofilin in combination with empty EGFP or EGFP-full length-p21 or EGFP-ΔNLS-p21 as indicated. After 30 h, cells were treated with 10 μM Y27632 for 5 h. The lysates were then electrophoresed and blotted with anti-phosphocofilin, anti-cofilin, and anti-p21 antibodies.

ing evidence that Akt, which acts downstream of PI3K, directly phosphorylates p21, thereby resulting in the cytoplasmic localization by causing nuclear export and increased stability of p21 in the cytoplasm (6, 34, 35). Therefore, we sought to determine whether inhibition of PI3K also affects cytoplasmic localization of p21 in Ras-transformed NIH3T3 cells. Treatment of cells with LY294002 caused a loss of cytoplasmic p21 within 2 h in 75% (75/100) of cells (Fig. 5A). We also detected, by Western blot, a decrease in the amount of p21 protein following the treatment of LY294002 (Fig. 5B). This down-regulation can be explained in part by proteasome-dependent degradation, because pretreatment of proteasome inhibitors, such as lactacystin and MG-132, prevented decrease of p21 caused by PI3K inhibition (data not shown). Furthermore, we found that inhibition of PI3K was also accompanied by the restoration of cofilin phosphorylation (Fig. 5B). However, inhibition of PI3K failed to induce reversion of stress fibers and focal adhesions (Fig. 1A), suggesting that restoration of cofilin phosphorylation in Ras-transformed cells is not sufficient for the reorganization of actin cytoskeleton but requires additional factors. See details under "Discussion."

DISCUSSION

Previous studies have shown that RhoA is required for Ras-mediated transformation (36). In the present study, we found that the level of active RhoA-GTP was increased in Ras-transformed NIH3T3 cells, which is consistent with recent studies done by others in different types of Ras-transformed cells (24, 29, 37). However, paradoxically, while RhoA is activated, the formation of stress fibers and focal adhesions is severely compromised in Ras-transformed NIH3T3 cells, implying that RhoA activity is no longer coupled via its interaction with ROCK to the formation of stress fibers. Previously, it was proposed that MEK-dependent down-regulation of ROCK-I/II proteins in Ras-transformed cells may represent a way for uncoupling Rho-GTP from ROCK (23, 24). However, such a

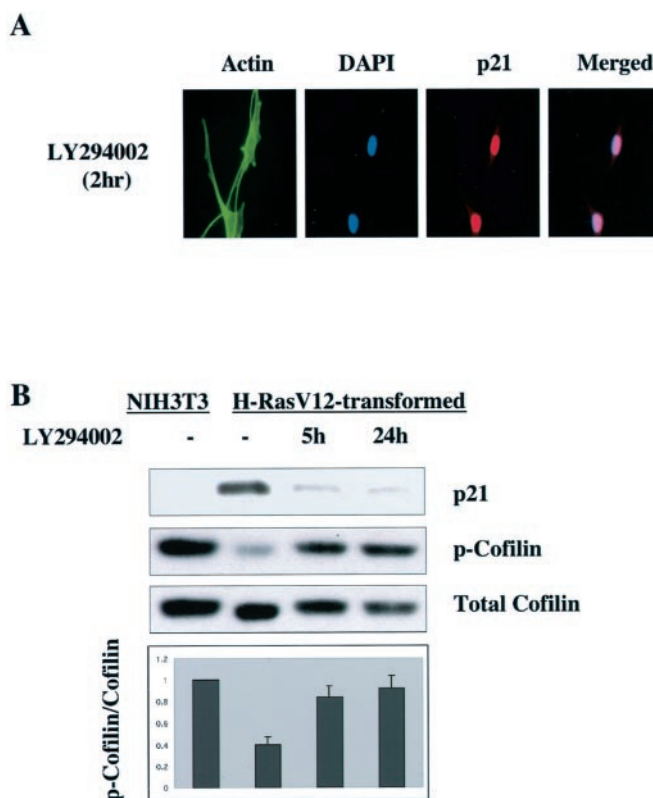


FIG. 5. Inhibition of PI3K leading to restoration of cofilin phosphorylation is not sufficient for stress fiber formation. Parental NIH3T3 and Ras-transformed cells were grown overnight and then treated with Me₂SO (0.1% v/v) or 50 μM LY294002 for the indicated times. *A*, Ras-transformed cells treated with LY294002 (2 h) were fixed and stained with Oregon green-conjugated phalloidin, DAPI, and anti-p21 antibody. *B*, whole cell lysates were analyzed by Western blot with anti-p21, anti-phosphocofilin, and anti-cofilin antibodies. Immunoblot for total cofilin were performed after membrane stripping. Relative levels of cofilin phosphorylation were measured by Western blot, as described in the legend to Fig. 2.

decrease of ROCK-I/II proteins was not detected in the present study (Fig. 1C), suggesting that there is another mechanism for uncoupling RhoA-GTP from activating Rho kinases.

Despite its role as a cell cycle inhibitor, p21 has been shown to be up-regulated in cell lines transformed by diverse oncoproteins as well as in many human cancers (2, 3, 32, 38). The functional significance of overexpression of p21 in tumorigenesis was supported in a study where introduction of antisense p21 oligodeoxynucleotides into nude mice that had been implanted with highly metastatic breast cancer cells resulted in suppression of tumor growth and angiogenesis, implicating a novel function of p21 as an oncogenic factor rather than a tumor suppressor (39). Although the mechanism by which up-regulation of p21 contributes to tumorigenesis remains unclear, one hypothesis is that p21 not only acts as a direct inhibitor of CDK2 (5, 40), but also functions as a scaffolding protein for the assembly of active cyclin D-CDK4/6 complex (41). As a consequence, the pool of increased p21 is sequestered in cyclin D-CDK4/6 complex thereby allowing increased activity of cyclin E-CDK2 for cell cycle progression (42). Recent studies provide evidence that, in addition to its role in regulating nuclear events, relocalization of p21 from the nucleus to the cytoplasm in cancer cells may have functions which are unrelated to its role as a CDK inhibitor (2, 3). For example, one clinical study has shown that p21 was predominantly cytoplasmic in the majority of breast cancers and it was closely associated with poor prognosis (11). Subsequent studies demonstrated that phosphorylation of p21 by Akt leads to the

cytoplasmic accumulation by causing nuclear export and increased stability of p21 in the cytoplasm (6, 34, 35). In agreement with this observation, we detected a complete loss of cytoplasmic p21 in Ras-transformed NIH3T3 cells within 2 h following the inhibition of PI3K, an upstream effector of Akt (Fig. 5A). Furthermore, total p21 proteins was barely detectable 5 h after PI3K inhibition (Fig. 5B). It was previously shown that the Raf/MEK/ERK pathway is responsible for the elevation of p21 mRNA transcription in H-Ras-transformed NIH3T3 cells (33). In agreement with these results, we found that inhibition of MEK by U0126 resulted in down-regulating the expression of total p21 protein (Fig. 2A). These decreases in the p21 protein by either U0126 or LY294002 were prevented when cells were pretreated with lactacystin or MG-132 (data not shown), suggesting that the stability of p21 protein is controlled by proteasome-dependent degradation. Collectively, these results demonstrate that both MEK-dependent and PI3K-dependent signaling pathways in Ras-transformed cells are necessary for *de novo* synthesis of p21, increased stability of p21 and localization of p21 protein to the cytoplasm (6, 33–35). Recently, it was reported that cyclin D1 is a critical mediator of Ras-induced p21 stability (32). In this report, they proposed that high level of cyclin D1 blocks p21 binding to the C8 α subunit of 20 S proteasome, thereby preventing p21 degradation. We also found that cyclin D1 is highly up-regulated in Ras-transformed NIH3T3 cells and the increase was abolished by either U0126 or LY294002 (data not shown).

What might be the functional role of elevated cytoplasmic p21, other than cell cycle control, in Ras-transformed cells? It was recently reported that p21, which is induced in the cytoplasm during the course of neuronal differentiation, regulates Rho-induced actin remodeling leading to neurite outgrowth phenotype (8). Prompted by this finding, we have investigated if cytoplasmic p21 plays a role in remodeling of the actin cytoskeleton in Ras-transformed NIH3T3 cells. To determine whether elevated cytoplasmic p21 inhibits the ROCK/LIMK/cofilin pathway, we used an antibody that detects cofilin phosphorylation by LIM kinase at Ser-3 residue. Here we demonstrate that accumulation of p21 lacking the NLS was sufficient to inhibit cofilin phosphorylation and to block ROCK-dependent formation of stress fibers (Figs. 3C and 4B). As previously shown by Tanaka *et al.* (8), we found that endogenous p21 in Ras-transformed cells forms a complex with ROCK-I *in vivo*, suggesting that p21 exerts its effect via binding to ROCK and inhibiting its downstream signaling (Fig. 4A). On the other hand, it is noteworthy that even though LY294002 caused restoration of cofilin phosphorylation (Fig. 5B), which was prevented when ROCK was inhibited by Y27632 (data not shown), inhibition of PI3K failed to reorganize the actin cytoskeleton (Fig. 1A). This suggests that restoration of the ROCK/LIMK/cofilin pathway alone is not sufficient to cause the formation of stress fibers. Consistent with this hypothesis, forced expressions of constitutively active or wild-type LIMK in Ras-transformed NIH3T3 did not result in restoration of stress fibers (data not shown). This result contrasts with what has been observed in Ras-transformed Swiss 3T3 fibroblasts (24), in which overexpression of LIMK was sufficient to cause the re-assembly of stress fibers. At present what factors are required in NIH3T3 cells, in addition to restoration of cofilin phosphorylation remains to be determined. One possibility is that expression of high molecular weight (HMW) tropomyosin (TM). The expression of HMW TMs has been reported to be suppressed in many transformed cells (43). Consistently, expression of HMW tropomyosins was barely detectable in Ras-transformed NIH3T3 cells (data not shown). In contrast, however, tropomyosin levels were not changed in Ras-transformed Swiss

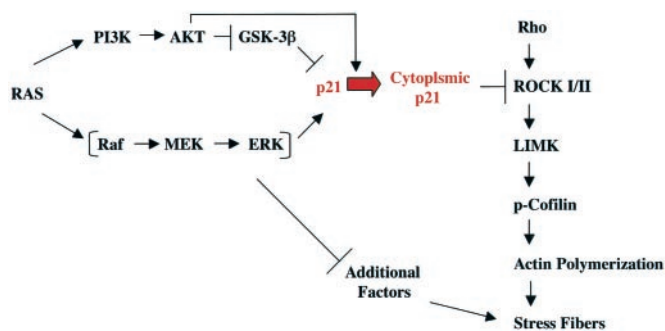


FIG. 6. Regulation of the Rho/ROCK/LIMK/cofilin pathway by p21^{Cip1} in Ras-transformed cells. Based on our findings and the work of others (6, 8, 33–35), a model can be proposed. We hypothesize that transformation of NIH3T3 cells by oncogenic Ras induces sustained activation of both PI3K and MEK-dependent pathways, which are necessary for the synthesis of p21, relocalization of p21 to the cytoplasm and increased stability of p21. The cytoplasmic p21 subsequently binds to ROCK and inhibits its downstream effector pathway thereby contributing to the loss of stress fibers. However, other cellular factors, in addition to restoring the ROCK/LIMK/cofilin pathway are required to fully restore stress fibers and focal adhesions. See details under “Discussion.”

3T3 cells (24). Interestingly, we found that restoration of stress fibers by MEK inhibition was accompanied by increased expressions of HMW TMs, TM-1 and TM-2. However, the increase of TMs was not detected when treated with LY294002 (data not shown). These might explain why ectopic expression of LIMK in Ras-transformed Swiss 3T3 cells was accompanied by formation of stress fibers (24), but we were unable to detect stress fiber induction following expression of wild-type or active LIMK in Ras-transformed NIH-3T3 cells. We also found that the inhibition of ROCK-dependent signaling either by dominant negative ROCK-I or Y-27632, in Ras-transformed cells, prevented restoration of stress fibers and focal adhesions caused by U0126 (data not shown). From these results, we hypothesize that restoration of ROCK/LIMK/cofilin pathway, via loss of cytoplasmic p21, is necessary but not sufficient for the stress fiber formation, and other additional factors, such as tropomyosins, that were not restored following inhibition of the PI3K pathway, are required (Fig. 6). Work is currently in progress to identify these factors.

In addition to a role for cytoplasmic p21, there is increasing evidence supporting a critical role for cytoplasmic p27^{Kip1}, another CDK inhibitor of Cip/Kip family, in regulation of cytoskeletal dynamics (3, 44, 48, 49). p27^{Kip1} like p21^{Cip1} can also be phosphorylated by AKT, which leads to its localization to the cytoplasm (45–47). In addition to our study and Tanaka and colleague’s (8) implicating a role of cytoplasmic p21 in actin remodeling, a role for cytoplasmic p27 in regulating cell motility has been reported (48). Accordingly, treatment of cells with hepatocyte growth factor (HGF) signaling resulted in phosphorylation on Ser-10 of p27^{Kip1} coupled with nuclear export of p27^{Kip1} to the cytoplasm, where it is required for cell motility through actin cytoskeletal rearrangement. Interestingly, analogous to mammalian cells, α -factor treatment of yeast cell causes cytoplasmic localization of Far1 protein, a cyclin-CDK inhibitor, followed by reorientation of the actin cytoskeleton and a polarized structure toward its mating partner (48, 49). Recently, it was reported that an increase of Cdc2 (CDK1) in prostate cancer cells modulates cell migration via specific association with caldesmon, a previously identified substrate of Cdc2, in membrane ruffles in motile cells (50, 51). Thus, in addition to the well-characterized functions of CDKs or CDK inhibitors as cell cycle regulators, they also have a direct role in the regulation of the actin cytoskeleton.

In conclusion, our studies demonstrate that expression of

cytoplasmic p21^{Cip1} is an essential factor in the signaling pathways that contribute to Ras-induced actin cytoskeletal remodeling. Further characterization of the pathways linking p21^{Cip1} to actin-mediated cellular functions will be critical to understand the morphological effects of various oncogenes. Finally, these studies suggest that localization of p21^{Cip1} to the cytoplasm in transformed cells may be involved in pathways that favor not only cell proliferation, but also cell motility thereby contributing to invasion and metastasis.

Acknowledgments—We thank Dr. James Bamburg of Colorado State University for providing EGFP-cofilin cDNA construct and Dr. Minoru Asada for supplying us with EGFP-full-p21 and EGFP-ΔNLS-p21. We also thank Dr. Jian Du and Yvette Seger in the Hannon laboratory for providing polyclonal anti-ROCK-I antibody and pWZL-H-RasV12 cDNA construct, respectively. Special thanks to Dr. Yuri Lazebnik, Dr. Senthil Muthuswamy, and Dr. Geraldine Pawlak for critical comments and helpful discussions regarding this manuscript.

REFERENCES

- Sherr, C. J., and Roberts, J. M. (1999) *Genes Dev.* **13**, 1501–1512
- Roninson, I. B. (2002) *Cancer Letts.* **179**, 1–14
- Coqueret, O. (2003) *Trends Cell Biol.* **13**, 65–70
- Alpan, R. S., and Pardee, A. B. (1996) *Cell Growth Differ.* **7**, 893–901
- Harper, J. W., Adami, G. R., Wei, N., Keyomarsi, K., and Elledge, S. J. (1993) *Cell* **75**, 805–816
- Zhou, B. P., Liao, Y., Xia, W., Spohn, B., Lee, M.-H., and Hung, M.-C. (2001) *Nat. Cell Biol.* **3**, 245–252
- Asada, M., Yamada, T., Ichijo, H., Delia, D., Miyazono, K., Fukumuro, K., and Mizutani, S. (1999) *EMBO J.* **18**, 1223–1234
- Tanaka, H., Yamashita, T., Asada, M., Mizutani, S., Yoshikawa, H., and Tohyama, M. (2002) *J. Cell Biol.* **158**, 321–329
- Biankin, A. V., Kench, J. G., Morey, A. L., Lee, C.-S., Biankin, S. A., Head, D. R., Hugh, T. B., Henshall, S. M., and Sutherland, R. L. (2001) *Cancer Res.* **61**, 8830–8837
- Korkolopoulou, P., Konstantinidou, A. E., Thomas-Tzagli, E., Christodoulou, P., Kapralos, P., and Davaris, P. (2000) *Appl. Immunohistochem. Mol. Morphol.* **8**, 285–292
- Winters, Z. E., Hunt, N. C., Bradburn, M. J., Royds, J. A., Turley, H., Harris, A. L., and Norbury, C. J. (2001) *Eur. J. Cancer* **37**, 2405–2412
- Jung, J. M., Bruner, J. M., Ruan, S., Langford, L. A., Kyritsis, A. P., Kobayashi, T., Levin, V. A., and Zhang, W. (1995) *Oncogene* **11**, 2021–2028
- Orend, G., Hunter, T., and Ruoslahti, E. (1998) *Oncogene* **16**, 2575–2583
- Bar-sagi, D., and Hall, A. (2000) *Cell* **103**, 227–238
- Amano, M., Fukata, Y., and Kaibuchi, K. (2000) *Exp. Cell Res.* **261**, 44–51
- Amano, M., Ito, M., Kimura, K., Fukata, Y., Chihara, K., Nakano, T., Matsura, Y., and Kaibuchi, K. (1996) *J. Biol. Chem.* **271**, 20246–20249
- Kimura, N., Ito, M., Amano, M., Chihara, K., Fukata, Y., Nakafuku, M., Yamamori, B., Feng, J., Nakano, T., Okawa, K., Iwamatsu, A., and Kaibuchi, K. (1996) *Science* **273**, 245–248
- Maekawa, M., Ishizaki, T., Boku, S., Watanabe, N., Fujita, A., Iwamatsu, A., Obinata, T., Ohashi, K., Mizuno, K., and Narumiya, S. (1999) *Science* **285**, 895–898
- Hunter, T. (1997) *Cell* **88**, 333–346
- Bondy, G. P., Wilson, S., and Chambers, A. F. (1985) *Cancer Res.* **45**, 6005–6009
- Fox, P. L., Sa, G., Dobrowolski, S. F., and Stacey, D. W. (1994) *Oncogene* **9**, 3519–3526
- Pawlak, G., and Helfman, D. M. (2001) *Curr. Opin. Gene Dev.* **11**, 41–47
- Pawlak, G., and Helfman, D. M. (2002) *Mol. Biol. Cell.* **13**, 336–347
- Sahai, E., Olson, M. F., and Marshall, C. J. (2001) *EMBO J.* **20**, 755–766
- Wood, K. W., Sarnecki, C., Roberts, T. M., and Blenis, J. (1992) *Cell* **92**, 1041–1050
- Rodriguez-Viciano, P., Warme, P. H., Khwaja, A., Marte, B. M., Pappin, D., Das, P., Waterfield, M. D., and Downward, J. (1997) *Cell* **89**, 457–467
- Kikuchi, A., Demo, S. D., Ye, Z. H., Chen, Y. W., and Williams, L. T. (1994) *Mol. Cell Biol.* **14**, 7483–7491
- Ren, X., Kioussis, W. B., and Schwartz, M. A. (1999) *EMBO J.* **18**, 578–585
- Chen, J. C., Zhuang, S., Nguyen, T. H., Boss, G. R., and Pilz, R. B. (2003) *J. Biol. Chem.* **278**, 2807–2818
- Bamburg, J. R., Mcgough, A., and Ono, S. (1999) *Trends Cell Biol.* **9**, 364–370
- Ohashi, K., Nagata, K., Maekawa, M., Ishizaki, T., Narumiya, S., and Mizuno, K. (2000) *J. Biol. Chem.* **275**, 3577–3582
- Coleman, M. L., Marshall, C. J., and Olson, M. F. (2003) *EMBO J.* **22**, 2036–2046
- Gartel, A. L., Najmabadi, F., Goufman, E., and Tyner, A. L. (2000) *Oncogene* **19**, 961–964
- Rossig, L., Badorff, C., Holzmann, Y., Zeiber, A. M., and Dimmeler, S. (2002) *J. Biol. Chem.* **277**, 9684–9689
- Li, Y., Dowbenko, D., and Lasky, L. A. (2002) *J. Biol. Chem.* **277**, 11352–11361
- Sahai, E., and Marshall, C. J. (2002) *Nature Reviews Cancer* **2**, 133–142
- Zondag, G. C., Evers, E. E., ten Klooster, J. P., Janssen, L., van der Kammen, R. A., and Collard, J. G. (2000) *J. Cell Biol.* **149**, 775–782
- Sinibaldi, D., Wharton, W., Turkson, J., Bowman, T., Pledger, W. J., and Jove, R. (2000) *Oncogene* **19**, 5419–5427
- Weiss, R. H., Marshall, D., Howard, L., Corbacho, A. M., Cheung, A. T., and Sawai, E. T. (2003) *Cancer Letts.* **189**, 39–48
- Noda, A., Ning, Y., Venable, S. F., Pereira-Smith, O. M., and Smith, J. R. (1994) *Exp. Cell Res.* **211**, 90–98
- Labauer, J., Garrett, M. D., Stevenson, L. F., Slingerland, J. M., Sandhu, C., Chou, H. S., Fattaey, A., and Harlow, E. (1997) *Genes Dev.* **11**, 847–862
- Winston, J., Dong, F., and Pledger, W. J. (1996) *J. Biol. Chem.* **271**, 11253–11260
- Ben-Ze'ev, A. (1997) *Curr. Opin. Cell Biol.* **9**, 99–108
- Liang, J., and Slingerland, J. M. (2003) *Cell Cycle* **2**, A48–A54
- Viglietto, G., Motti, M. L., Bruni, P., Mellilo, R. M., D'alesio, A., Califano, D., Vinci, F., Chiappetta, G., Tschlis, P., Bellacosa, A., Fusco, A., and Santoro, M. (2002) *Nat. Med.* **8**, 1136–1144
- Liang, J., Zubovitz, J., Petrocelli, T., Kotchetkov, R., Connor, M. K., Han, K., Lee, J. H., Ciarallo, S., Catzavelos, C., Beniston, R., Franssen, E., and Slingerland, J. M. (2002) *Nat. Med.* **8**, 1153–1160
- Shin, I., Yakes, F. M., Rojo, F., Shin, N. Y., Bakin, A. V., Baselga, J., and Arteaga, C. L. (2002) *Nat. Med.* **8**, 1145–1152
- Mcallister, S. S., Becker-Hapak, M., Pintucci, G., pagano, M., and Dowdy, S. F. (2003) *Mol. Cell Biol.* **23**, 216–228
- Gulli, M. P., and Peter, M. (2001) *Genes Dev.* **15**, 365–379
- Manes, T., Zheng, D.-Q., Tognin, S., Woodard, A. S., Marchisio, P. C., and Languino, L. R. (2003) *J. Cell Biol.* **161**, 817–826
- Yamashiro, S., Yamakita, Y., Hosoya, H., and Matsumura, F. (1991) *Nature* **349**, 169–172